

Secondary magnetic inclusions in detrital zircons from the Jack Hills, Western Australia, and implications for the origin of the geodynamo

Benjamin P. Weiss¹, Roger R. Fu², Joshua F. Einsle^{3,4}, David R. Glenn^{5,6}, Pauli Kehayias^{5,6}, Elizabeth A. Bell⁷, Jeff Gelb⁸, Jefferson F.D.F. Araujo^{1,9}, Eduardo A. Lima¹, Cauê S. Borlina¹, Patrick Boehnke^{10,11}, Duncan N. Johnstone⁴, T. Mark Harrison⁷, Richard J. Harrison³, and Ronald L. Walsworth^{5,6}

¹Department of Earth, Atmospheric, and Planetary Sciences, Massachusetts Institute of Technology, Cambridge, Massachusetts 02139, USA

²Department of Earth and Planetary Sciences, Harvard University, Cambridge, Massachusetts 02138, USA

³Department of Earth Sciences, University of Cambridge, Cambridge CB2 3EQ, UK

⁴Department of Materials Science and Metallurgy, University of Cambridge, Cambridge CB3 0FS, UK

⁵Harvard-Smithsonian Center for Astrophysics, Cambridge, Massachusetts 02138, USA

⁶Department of Physics, Harvard University, Cambridge, Massachusetts 02138, USA

⁷Department of Earth, Planetary, and Space Sciences, University of California, Los Angeles, California 90095, USA

⁸Carl Zeiss X-ray Microscopy Inc., Pleasanton, California 94588, USA

⁹Department of Physics, Pontifical Catholic University of Rio de Janeiro, Rio de Janeiro 22451-900, Brazil

¹⁰Department of the Geological Sciences, University of Chicago, Chicago, Illinois 60637, USA

¹¹Chicago Center for Cosmochemistry, Chicago, Illinois 60637, USA

ABSTRACT

The time of origin of Earth's dynamo is unknown. Detrital zircon crystals containing ferromagnetic inclusions from the Jack Hills of Western Australia have the potential to contain the oldest records of the geodynamo. It has recently been argued that magnetization in these zircons indicates that an active dynamo existed as far back as 4.2 Ga. However, the ages of ferromagnetic inclusions in the zircons are unknown. Here we present the first detailed characterization of the mineralogy and spatial distribution of ferromagnetic minerals in Jack Hills detrital zircons. We demonstrate that ferromagnetic minerals in most Jack Hills zircons are commonly located in cracks and on the zircons' exteriors. Hematite is observed to dominate the magnetization of many zircons, while other zircons also contain significant quantities of magnetite and goethite. This indicates that the magnetization of most zircons is likely to be dominantly carried by secondary minerals that could be hundreds of millions to billions of years younger than the zircons' crystallization ages. We conclude that the existence of the geodynamo prior to 3.5 Ga has yet to be established.

INTRODUCTION

The unknown early history of Earth's magnetic field has important implications for our understanding of the planet's thermal evolution and the process of dynamo generation. In particular, inner core crystallization, the likely power source for today's dynamo, is thought to have only initiated at <1.5 Ga (Davies et al., 2015). Therefore, identification of an early field would indicate that the core was stirred by other power sources, such as precipitation of Mg (O'Rourke and Stevenson, 2016), or perhaps that the dynamo was generated by exotic processes like a convecting basal magma ocean (Ziegler and Stegman, 2013). Furthermore, because Earth's field controls the penetration of the solar-wind electric field into the ionosphere, the dynamo's history may have strongly influenced Earth's water budget and oxidation state (Tarduno et al., 2014).

Although paleomagnetic studies of Archean rocks indicate that a dynamo with an intensity of at least half that of the present day existed by

3.45 Ga (Tarduno et al., 2014), the earlier history of the field is uncertain. With U-Pb ages ranging from ca. 3.0 Ga to 4.38 Ga (Holden et al., 2009), detrital zircon crystals from the Jack Hills of Western Australia have the potential to retain geodynamo records from the missing first billion years of Earth's history. Although zircon is itself not ferromagnetic, magnetization could be carried by ferromagnetic inclusions within the zircons (Fu et al., 2017; Sato et al., 2015).

It was recently proposed that the Jack Hills zircons contain records of the dynamo dating back to their oldest U-Pb crystallization ages of 4.2 Ga (Dare et al., 2016; Tarduno et al., 2015). However, it is currently unknown whether these zircons have escaped thermal and chemical remagnetization during the intervening time since their formation. In fact, many Jack Hills rocks were pervasively remagnetized sometime after 3.0 Ga (Weiss et al., 2015) (Appendix DR1 in the GSA Data Repository¹). Although Tarduno et al. (2015) conducted a "micro-conglomerate test" in an attempt to demonstrate a lack of post-depositional remagnetization, this employed 0.5–0.8-mm-size specimens consisting predominantly of quartzite pebble material enclosing zircons with sizes of just 0.2–0.3 mm. As such, the result of their test rests on the unverified assumption that the magnetization of the specimens is dominated by inclusions within the embedded zircon. Furthermore, although Tarduno et al. (2015) and Bono et al. (2018) argued that thermal remagnetization of the zircons would have resulted in Pb/U variations during secondary ion mass spectrometry (SIMS) depth-profiling that they did not observe, their instrumentation should have been incapable of detecting such variations (Weiss et al., 2016). In any case, even if such variations could have been detected by Tarduno et al. (2015), such Pb/U depth-profiling is not a sensitive test for thermal remagnetization because of lead's extremely low diffusivity at 600 °C in non-metamict zircons under both dry and hydrous conditions (Cherniak and Watson, 2003).

¹GSA Data Repository item 2018135, Figures DR1–DR12, Tables DR1–DR4, Movie DR1, and Appendices DR1–DR3, is available online at <http://www.geosociety.org/datarepository/2018/> or on request from editing@geosociety.org.

Along with demonstrating a lack of thermal remagnetization, another key requirement for establishing that the bulk natural remanent magnetization (NRM) of a zircon crystal is a robust indicator of magnetic fields at the time of zircon crystallization is the demonstration that its ferromagnetic inclusions are dominantly primary rather than alteration products of primary inclusions or deposits in cracks and voids. Here we characterize the ferromagnetic mineral assemblage in Jack Hills zircons using compositional and magnetic analyses to assess whether magnetization in most Jack Hills zircons is carried dominantly by primary or secondary inclusions.

METHODS

We sought to identify the ferromagnetic mineralogy of the zircon inclusions, establish whether they are primary or secondary by focusing on their relationships to cracks and alteration textures, and test the efficacy of acid-washing for removing secondary inclusions. We conducted magnetic, compositional, and mineralogical analyses on 11 sets of Jack Hills detrital zircons (425 total zircons newly analyzed in this study, along with re-analysis of 2450 zircons previously studied by Bell et al. [2015]; Table DR1) from quartz pebble conglomerates sampled at the Erawandoo Hill Hadean-zircon discovery outcrop [site W74 of Weiss et al. (2016, their figure S2)]. Eleven sets of zircons were mounted in several different ways for our magnetic measurements (Appendix DR2). We mapped the three components of the isothermal remanent magnetization (IRM) and NRM fields above 381 zircons using quantum diamond microscopy (QDM) (Fu et al., 2017; Glenn et al., 2017) (Appendix DR2). QDM employs optically addressable nitrogen vacancy centers in diamond that are sensitive to magnetic fields via the Zeeman effect. We also mapped the vertical component of the NRM field of 109 zircons at using superconducting quantum interference device (SQUID) microscopy (SM). SM enables ultra-sensitive measurements of net magnetic moments (Lima and Weiss, 2016; Fu et al. 2017). Curie temperatures of inclusions were estimated by SM mapping of thermal demagnetization of IRM.

Of the zircons imaged with QDM, 34 grains were subsequently analyzed with backscattered scanning electron microscopy (BSEM), energy dispersive spectroscopy (EDS), and wavelength dispersive spectroscopy (WDS). QDM is most sensitive to magnetic materials located up to tens of microns below the polished grain surfaces, while electron microscopy is only sensitive to the top $<2\ \mu\text{m}$ of the grains. Following these analyses, the three-dimensional Fe inclusion distribution in one zircon was then imaged using X-ray tomography using Carl Zeiss Xradia 520 Versa and Ultra XRM-L200 microscopes (spatial resolutions of 750 and 150 nm, respectively).

RESULTS

Zircons Not Treated with Concentrated Acid

We begin by discussing zircons not washed with acid and those washed with weak (0.5 N) HCl (Table DR1). SM measurements show that non-acid-washed zircons from set 4 have a mean NRM of $8.3 \times 10^{-13}\ \text{Am}^2$, 23% of which are $>1 \times 10^{-12}\ \text{Am}^2$ (Fig. DR10A; Table DR3). QDM imaging of non-acid-washed zircons from set 1 carrying IRM (Fig. DR3) and set 3 carrying NRM (Figs. DR4A–DR4D) was conducted on 261 zircons in a lower-sensitivity reconnaissance mode followed by higher-sensitivity imaging of 84 selected zircons (see Glenn et al. [2017] and Table DR2). Of the 147 and 76 such zircons detected in the reconnaissance and higher-sensitivity modes, respectively, 122 (83%) and 55 (72%) respectively, exhibited magnetic anomalies centered on locations that are within $\sim 20\ \mu\text{m}$ of the grains' exteriors (Figs. 1A–1C; Figs. DR1A–DR1J; bottom grains in Figs. DR4A, DR4C, and DR4D). We observed similar results for zircons washed with 0.5 N HCl (i.e., sets 5 and 6): 67% of the 9 zircons detected with QDM showed exterior-only NRM (bottom grains in Figs. DR4E and DR4J; and both grains in Figs. DR4G and DR4I). Of the 23 non-acid-washed and 0.5 N HCl-washed zircons analyzed with

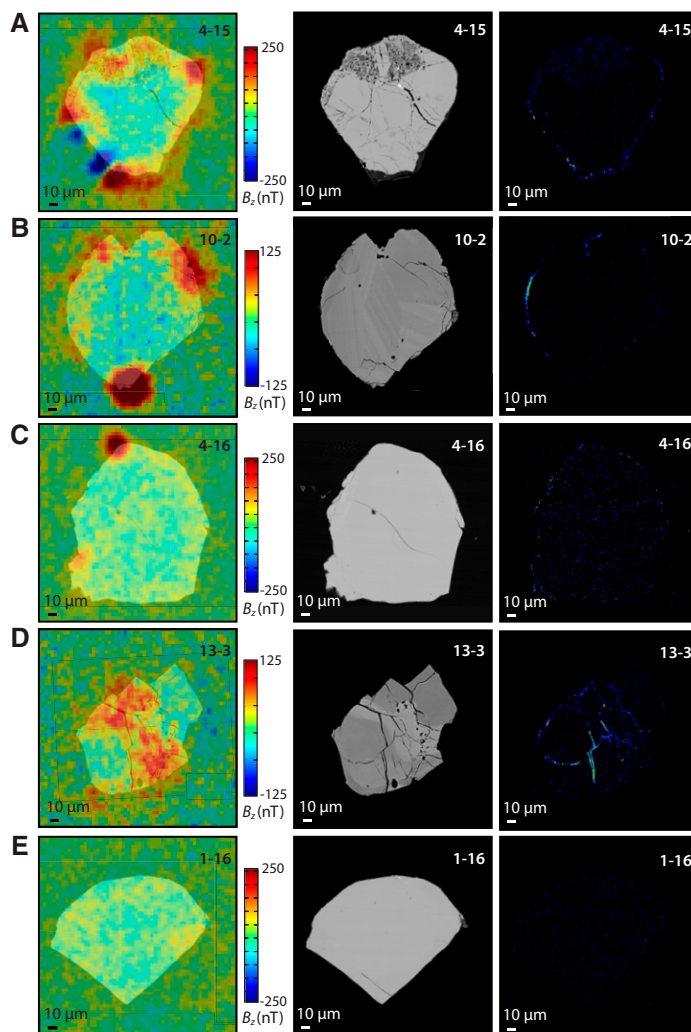


Figure 1. Magnetization, texture, and composition of Jack Hills (Western Australia) zircons not washed with acid (i.e., set 1). Shown are quantum diamond microscopy (QDM) maps of the vertical component of the magnetic field at $\sim 1\text{--}10\ \mu\text{m}$ above the samples overlain on backscattered electron microscopy (BSEM) images (left), BSEM images (middle), and maps of Fe abundance from wavelength dispersive spectroscopy (WDS) (right). A: Zircon RSES 199–4–15 (RSES—Australian National University Research School of Earth Sciences) (Pb–Pb age of $<3900\ \text{Ma}$). B: Zircon RSES 199–10–2 (Pb–Pb age of $4050 \pm 8\ \text{Ma}$). C: Zircon RSES 199–4–16 (Pb–Pb age of $3973 \pm 8\ \text{Ma}$). D: Zircon RSES 199–13–3 (Pb–Pb age $<3900\ \text{Ma}$). E: Zircon RSES 199–1–16 (Pb–Pb age $<3900\ \text{Ma}$). See Figures DR1 and DR2 (see footnote 1) for more QDM and BSEM analyses of set 1 zircons, and see Figure DR2 for QDM data on all set 1 zircons and for magnetic field scale bar. See Table DR4 for the Pb–Pb ages of these zircons.

WDS, 91% (including 93% of the 15 zircons with exterior-only magnetic sources) have secondary Fe-rich rinds located within $<5\ \mu\text{m}$ of the grain exteriors (Figs. 1A–1C; Figs. DR1A, DR1B, DR1D–DR1J, DR2, DR5, and DR6). These rinds have thicknesses ranging from $<2\ \mu\text{m}$ for most zircons (e.g., Figs. 1B–1D) and up to $10\ \mu\text{m}$ for one zircon (e.g., Fig. DR1). Additionally, X-ray tomography of an uncracked, optically clear Hadean zircon with exterior-only magnetic sources, which showed no sign of secondary mineralization based on optical inspection, identified high-X-ray absorption grains (consistent with Fe-rich materials) exclusively on the zircon exterior (Fig. 2). The spatial association of magnetic anomalies and Fe-rich secondary materials suggests that the latter carry most of the magnetization in these zircons. Although some exterior magnetic anomalies are not associated with Fe-rich materials detectable with

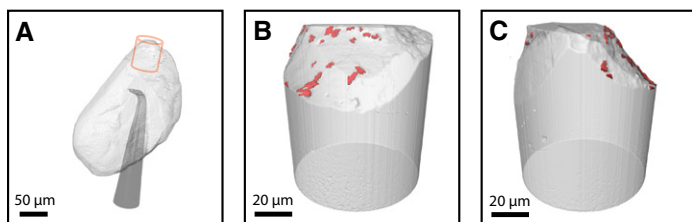


Figure 2. X-ray tomography of a Jack Hills (Western Australia) zircon not washed with acid (i.e., set 1). Zircon RSES 199–1–15 (RSES—Australian National University Research School of Earth Sciences) and has a U-Pb age of 4019 ± 5 Ma. **A:** Tomogram from Xradia 520 Versa showing entire grain (light gray) on mount (dark hook). Cylinder shows location of tomograms in B and C. **B, C:** Orthogonal views from Ultra XRML200 microscope. Red voxels have high X-ray absorption relative to that of zircon host (gray) and are inferred to be Fe-rich particles. See Movie DR1 (see footnote 1) for renderings of these data from other viewpoints, and Fig. DR2C for maps of this zircon's magnetic field.

WDS (e.g., anomaly at upper right of grain in Figure 1B), the difference in depth sensitivity between these techniques (see Methods) implies that many of these anomalies may be likely associated with secondary Fe-rich materials located $>2 \mu\text{m}$ beneath the polished grain surfaces.

We found that just 21% of detected zircon grains not washed with strong HCl contain interior magnetic sources (i.e., that lie deeper than $20 \mu\text{m}$ from the rim) (e.g., Fig. 1D; Figs. DR1M–DR1P; Table DR2). Although the bulk magnetizations of the latter zircons are better candidates for being dominantly carried by primary ferromagnetic materials, the exteriors of many of these zircons nevertheless carry substantial magnetization (e.g., Fig. 1D; Figs. DR1M–DR1P). In particular, 100% (5 out of 5) these zircons with interior magnetic sources analyzed with electron microscopy have Fe-rich rinds (e.g., Fig. 1D; Figs. DR1M, DR1O, and DR1P). Furthermore, we found that 100% (5 out of 5) of these zircons analyzed with electron microscopy host Fe-rich secondary minerals in interior cracks and metamict zones (e.g., Fig. 1D; Figs. DR1M, DR1O, and DR1P). QDM maps of the zircon host conglomerate found that the IRM of in situ zircons is significantly weaker than that associated with quartz grain boundaries that are commonly filled Fe oxides (Fig. DR7). Therefore, until it is demonstrated that the NRM of the Tarduno et al. (2015) micro-conglomerate test samples are dominated by primary inclusions in the zircon rather than by the surrounding rock, the outcome of that test should be regarded as uncertain.

Raman spectroscopy indicates the presence of hematite in at least two zircons prior to any lab heating (Fig. DR8). Furthermore, SM measurements of thermal demagnetization of IRM (Fig. 3; Fig. DR9), found that 100% of 9 grains with clearly identified Curie temperatures contained hematite (Curie temperature 675°C) while 22% also contained magnetite (Curie temperature 580°C). These data also demonstrate that several zircons likely contain goethite (Curie temperatures $50\text{--}120^\circ\text{C}$) and possibly pyrrhotite (Curie temperature 325°C). During repeat heating experiments, it was observed that a zircon dominated by hematite during the first heating became dominated by magnetite during the second heating, indicating that heating severely altered the magnetization carriers (Fig. DR9C).

These observations collectively indicate that the NRM and IRM in most of our Jack Hills zircons not washed with concentrated HCl are predominantly carried by secondary Fe oxides deposited on the zircon exterior or within cracks and voids in the zircon interior. Our identification of hematite as a major remanence carrier contrasts with the observations of Tarduno et al. (2015), who found that essentially all of their analyzed zircons had remanence apparently dominated by magnetite. A possible explanation for this discrepancy is that hematite was originally present in the zircons of Tarduno et al. (2015), but was altered to magnetite by their heating experiments (e.g., Fig. DR9C) prior to their lowest-temperature checks for alteration (i.e., 550°C).

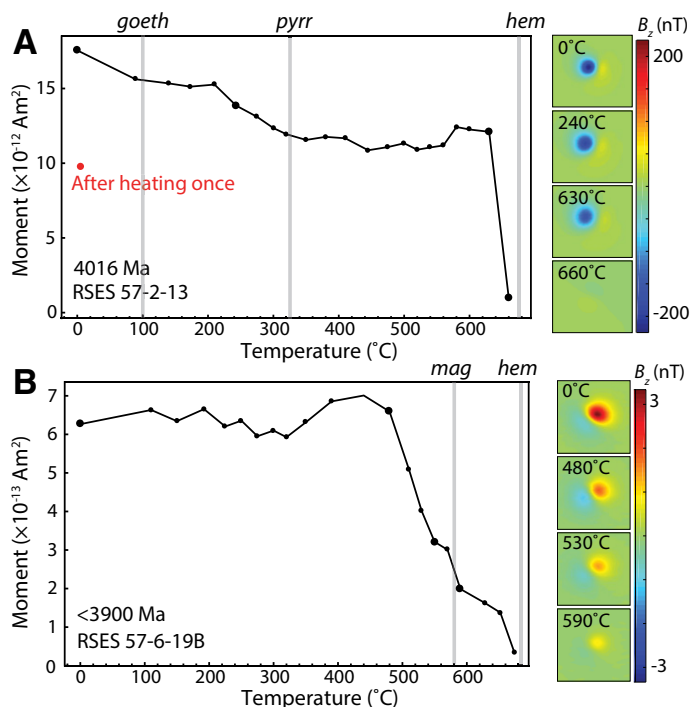


Figure 3. Thermal demagnetization of non-acid-washed Jack Hills (Western Australia) zircons carrying isothermal remanent magnetization (IRM) (i.e., set 2). Shown is the moment inferred from SQUID microscopy (SM) maps following each thermal demagnetization step (0°C denotes no heating). Red point indicates a second IRM experiment conducted after the zircons had been heated to 680°C . At right of each demagnetization curve are SM maps for selected demagnetization steps (large black circles). SM maps show the vertical component of the magnetic field $\sim 230 \mu\text{m}$ above the zircons. Both zircons were found to contain origin-trending, single-component IRMs. **A:** Zircon RSES 57–2–13 (RSES—Australian National University Research School of Earth Sciences) (Pb–Pb age 4016 ± 6 Ma). See Figure DR8 (see footnote 1) for Raman spectrum of this zircon, taken prior to laboratory heating, that identifies hematite. **B:** Fragment of zircon RSES 57–6–19 (Pb–Pb age <3900 Ma). See Figure DR7 for thermal demagnetization data of more Jack Hills zircons, including a second fragment from zircon in B.

Zircons Treated with Concentrated (6N) Acid

SM measurements of set 9 find that zircons washed in concentrated HCl have a mean NRM only 59% of that of non-acid-washed zircons (Fig. DR10B; Table DR3). Furthermore, only 12% of acid-washed zircons have moments $>1 \times 10^{-12} \text{Am}^2$. QDM measurements of sets 7 and 8 show that IRM is also weakened by acid-washing, with only 58% of such zircons detected (compared to 90% of unwashed set 1 zircons analyzed with QDM in the high-sensitivity mode).

Even so, QDM imaging showed that of the 14 zircons with detectable IRM, 29% still have magnetic sources confined largely to their exteriors (Fig. 4C; Fig. DR12A [both grains], and DR12C [bottom grain]). Furthermore, 36% of the 11 grains analyzed with EDS still have Fe-rich exterior rinds (Figs. 4B and 4C; Figs. DR11E and DR11H). Also, 100% of the 8 zircons analyzed with EDS and having interior magnetic sources contain Fe-rich cracks and alteration textures in their interiors (Figs. 4A and 4B; Figs. DR11A, DR11C–DR11G). Again, we cannot exclude the possibility that interior anomalies not associated with Fe-rich surface alteration visible in electron microscopy are instead associated with such alteration minerals below the polished surface. Overall, our analyses demonstrate that washing with concentrated HCl reduces the NRM and IRM of the zircons, particularly on the grain exteriors. Unfortunately, this often still leaves large quantities of Fe-rich alteration materials behind that could carry significant remanence. As described in Appendix DR3, these results are broadly consistent with the observations of Fe oxide inclusions by Bell et al. (2015).

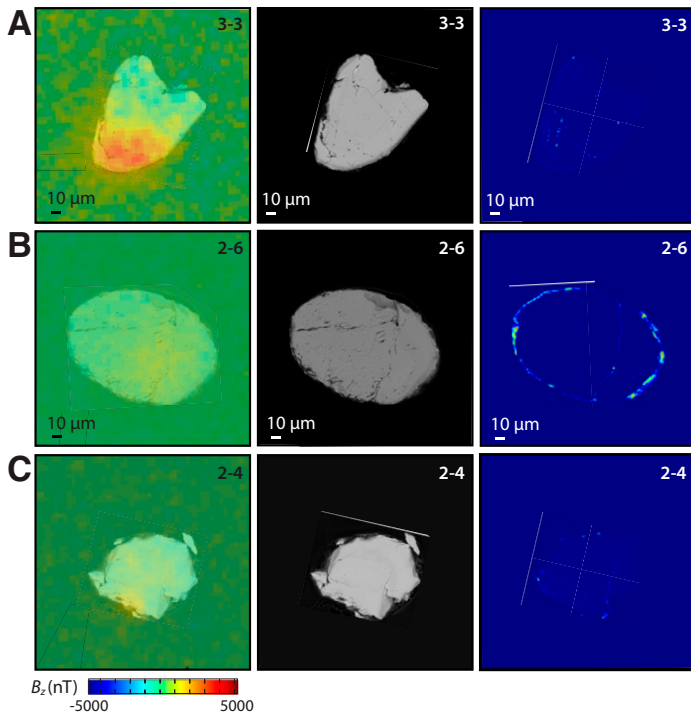


Figure 4. Magnetization, texture and composition of Jack Hills (Western Australia) zircons washed with 6 N HCl for 12 min (i.e., set 7) and 1 h (i.e., set 8). Shown are quantum diamond microscopy (QDM) maps of the vertical component of the magnetic field overlain on backscattered electron microscopy (BSEM) images (left), BSEM images (middle), and maps of Fe abundance from energy dispersive spectroscopy (EDS) (right). A: Zircon D175M-B1-3-3. B: Zircon D175M-B2-2-6. C: Zircon D175M-B2-2-4. See Figures DR11–DR13 (see footnote 1) for measurements of additional acid-washed zircons.

CONCLUSIONS

Collectively, our analyses indicate that most Jack Hills zircons not washed with concentrated HCl have NRM and IRM likely dominantly carried by secondary iron oxides, some of which are hematite. In particular, of 85 such zircons detected by QDM in its high-resolution mode, 72% have magnetic anomalies only observed at the exterior of the grains. All such zircons analyzed with electron microscopy were found to have Fe-rich secondary rinds. Furthermore, even the few zircons with interior magnetic sources were found to have spatially associated cracks containing Fe-rich alteration products. These minerals were apparently deposited on the zircons' exteriors or within voids in the zircons' interiors at an unknown time(s) over the past 3–4 b.y. since the zircons formed. Such alteration may have coincided with known thermal disturbances and/or aqueous alteration events at ca. 2.6, ca. 2.0, ca. 1.8, ca. 1.2, ca. 1.1, and ca. 0.8 Ga (summarized in Weiss et al., 2015), and/or during deep weathering over the past ~0.2 b.y. (Pidgeon et al., 2017). Consistent with this, nearly all monazite and xenotime inclusions in Jack Hills zircons, including those apparently entirely enclosed within uncracked regions, have U–Pb ages younger than 2.6 Ga, indicating they formed long after the zircons crystallized (Rasmussen et al., 2011). The state of Jack Hills zircon ferromagnetic inclusions differs greatly from that in 0.767 ka non-detrital zircons from the Bishop Tuff, which commonly are in the form of primary magnetite grains that dominate the stable NRM (Fu et al., 2017). We conclude that the ages of NRMs in previously studied Jack Hills zircons are unknown. As such, there currently is no robust evidence for a geodynamo active prior to the oldest known well-preserved rock record at 3.5 Ga.

ACKNOWLEDGMENTS

These analyses were supported by National Science Foundation grant EAR1647504, Thomas F. Peterson, Jr., and a Chamberlin Postdoctoral Fellowship to Boehnke.

We thank A. Steele for use of his Raman microscope and N. Chatterjee for assistance with the microprobe.

REFERENCES CITED

- Bell, E.A., Boehnke, P., Hopkins-Wielicki, M.D., and Harrison, T.M., 2015, Distinguishing primary and secondary inclusion assemblages in Jack Hills zircons: *Lithos*, v. 234–235, p. 15–26, <https://doi.org/10.1016/j.lithos.2015.07.014>.
- Bono, R.K., Tarduno, J.A., Dare, M.S., Mitra, R.D., and Cottrell, R.D., 2018, Cluster analysis on a sphere: Application to magnetizations from metasediments of the Jack Hills, Western Australia: *Earth and Planetary Science Letters*, v. 484, p. 67–80, <https://doi.org/10.1016/j.epsl.2017.12.007>.
- Cherniak, D.J., and Watson, E.B., 2003, Diffusion in zircon: *Reviews in Mineralogy and Geochemistry*, v. 53, p. 113–143, <https://doi.org/10.2113/0530113>.
- Dare, M.S., Tarduno, J.A., Bono, R.K., Cottrell, R.D., Beard, J.S., and Kodama, K.P., 2016, Detrital magnetite and chromite in Jack Hills quartzite cobbles: Further evidence for the preservation of primary magnetizations and new insights into sediment provenance: *Earth and Planetary Science Letters*, v. 451, p. 298–314, <https://doi.org/10.1016/j.epsl.2016.05.009>.
- Davies, C., Pozzo, M., Gubbins, D., and Alfè, D., 2015, Constraints from material properties on the dynamics and evolution of Earth's core: *Nature Geoscience*, v. 8, p. 678–685, <https://doi.org/10.1038/ngeo2492>.
- Fu, R.R., et al., 2017, Evaluating the paleomagnetic potential of single zircon crystals using the Bishop Tuff: *Earth and Planetary Science Letters*, v. 458, p. 1–13, <https://doi.org/10.1016/j.epsl.2016.09.038>.
- Glenn, D.R., Fu, R.R., Kehayias, P., Le Sage, D., Lima, E.A., Weiss, B.P., and Walsworth, R.L., 2017, Micrometer-scale magnetic imaging of geological samples using a quantum diamond microscope: *Geochemistry Geophysics Geosystems*, v. 18, <https://doi.org/10.1002/2017GC006946>.
- Holden, P., Lanc, P., Ireland, T.R., Harrison, T.M., Foster, J.J., and Bruce, Z., 2009, Mass-spectrometric mining of Hadean zircons by automated SHRIMP multi-collector and single-collector U/Pb zircon age dating: The first 100,000 grains: *International Journal of Mass Spectrometry*, v. 286, p. 53–63, <https://doi.org/10.1016/j.ijms.2009.06.007>.
- Lima, E.A., and Weiss, B.P., 2016, Ultra-high sensitivity moment magnetometry of geological samples using magnetic microscopy: *Geochemistry Geophysics Geosystems*, v. 17, <https://doi.org/10.1002/2016GC006487>.
- O'Rourke, J.G., and Stevenson, D.J., 2016, Powering Earth's dynamo with magnetite precipitation from the core: *Nature*, v. 529, p. 387–389, <https://doi.org/10.1038/nature16495>.
- Pidgeon, R.T., Nemchin, A.A., and Whitehouse, M.J., 2017, The effect of weathering on U–Th–Pb and oxygen isotope systems of ancient zircons from the Jack Hills, Western Australia: *Geochimica et Cosmochimica Acta*, v. 197, p. 142–166, <https://doi.org/10.1016/j.gca.2016.10.005>.
- Rasmussen, B., Fletcher, I.R., Muhling, J.R., Gregory, C.J., and Wilde, S.A., 2011, Metamorphic replacement of mineral inclusions in detrital zircon from Jack Hills, Australia: Implications for the Hadean Earth: *Geology*, v. 39, p. 1143–1146, <https://doi.org/10.1130/G32554.1>.
- Sato, M., Yamamoto, S., Yamamoto, Y., Okada, Y., Ohno, M., Tsunakawa, H., and Maruyama, S., 2015, Rock-magnetic properties of single zircon crystals sampled from the Tanzawa tonalitic pluton, central Japan: *Earth, Planets, Space*, v. 67, p. <https://doi.org/10.1186/s40623-40015-40317-40629>.
- Tarduno, J.A., Blackman, E.G., and Mamajek, E.E., 2014, Detecting the oldest geodynamo and attendant shielding from the solar wind: Implications for habitability: *Physics of the Earth and Planetary Interiors*, v. 233, p. 68–87, <https://doi.org/10.1016/j.pepi.2014.05.007>.
- Tarduno, J.A., Cottrell, R.D., Davis, W.J., Nimmo, F., and Bono, R.K., 2015, A Hadean to Paleoproterozoic geodynamo recorded by single zircon crystals: *Science*, v. 349, p. 521–524, <https://doi.org/10.1126/science.aaa9114>.
- Weiss, B.P., Maloof, A.C., Harrison, T.M., Swanson-Hysell, N.L., Fu, R.R., Kirschvink, J.L., Watson, E.B., Coe, R.S., Tikoo, S.M., and Ramezani, J., 2016, Reply to Comment on: "Pervasive remagnetization of detrital zircon host rocks in the Jack Hills, Western Australia and implications for records of the early dynamo": *Earth and Planetary Science Letters*, v. 450, p. 409–412, <https://doi.org/10.1016/j.epsl.2016.07.001>.
- Weiss, B.P., et al., 2015, Pervasive remagnetization of detrital zircon host rocks in the Jack Hills, Western Australia and implications for records of the early geodynamo: *Earth and Planetary Science Letters*, v. 430, p. 115–128, <https://doi.org/10.1016/j.epsl.2015.07.067>.
- Ziegler, L. B., and Stegman, D. R., 2013, Implications of a long-lived basal magma ocean in generating Earth's ancient magnetic field: *Geochemistry Geophysics Geosystems*, v. 14, <https://doi.org/10.1002/2013GC005001>.

Manuscript received 27 November 2017

Revised manuscript received 13 February 2018

Manuscript accepted 15 February 2018

Printed in USA